

The distribution of tree biomass carbon within the Pacific Coastal Temperate Rainforest, a disproportionally carbon dense forest

Trevor A. Carter Da and Brian Bumaab

^aDepartment of Integrative Biology, University of Colorado Denver, 1201 Larimer Street, Denver, CO 80203, USA; ^bEnvironmental Defense Fund, 2060 Broadway, Boulder, CO 80302, USA

Corresponding author: Trevor A. Carter (email: trevor.carter@ucdenver.edu)

Abstract

Spatially explicit global estimates of forest carbon storage are typically coarsely scaled. While useful, these estimates do not account for the variability and distribution of carbon at management scales. We asked how climate, topography, and disturbance regimes interact across and within geopolitical boundaries to influence tree biomass carbon, using the perhumid region of the Pacific Coastal Temperate Rainforest, an infrequently disturbed carbon dense landscape, as a test case. We leveraged permanent sample plots in southeast Alaska and coastal British Columbia and used multiple quantile regression forests and generalized linear models to estimate tree biomass carbon stocks and the effects of topography, climate, and disturbance regimes. We estimate tree biomass carbon stocks are either 211 (SD = 163) Mg C ha⁻¹ or 218 (SD = 169) Mg C ha⁻¹. Natural disturbance regimes had no correlation with tree biomass but logging decreased tree biomass carbon and the effect diminished with increasing time since logging. Despite accounting for 0.3% of global forest area, this forest stores between 0.63% and 1.07% of global aboveground forest carbon as aboveground live tree biomass. The disparate impact of logging and natural disturbance regimes on tree biomass carbon suggests a mismatch between current forest management and disturbance history.

Key words: disturbance regimes, forest carbon, forest disturbance, logging, tree biomass carbon

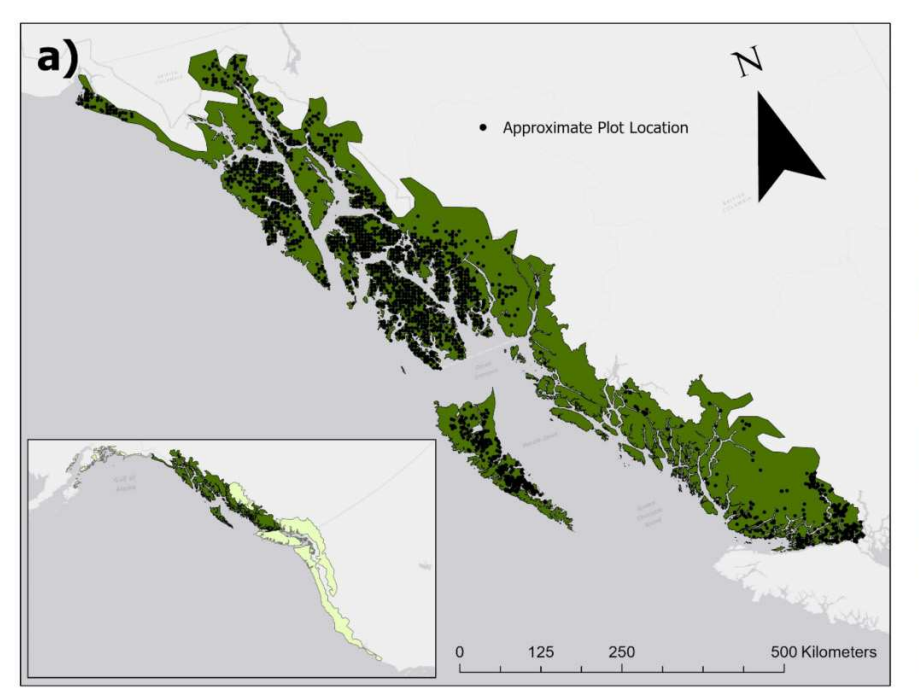
Introduction

Forested ecosystems are important contributors to the global carbon cycle (Litton et al. 2007; Pan et al. 2011) in part because of their ability to retain carbon for centuries to millennia. Global estimates of forest carbon pools vary between 234 and 363 Pg of carbon (Kindermann et al. 2008; Pan et al. 2011; Santoro et al. 2021). Although valuable, these widely available global estimates of forest carbon do not (nor are intended to) capture the variability and distribution of carbon at regional scales (McNicol et al. 2019); hence regional modeling is still necessary for many questions at management scales. To better account for forest carbon at regional and management scales, estimates and mapping efforts must incorporate appropriately scaled patterns and variability of the landscape, such as climatic and topographic processes that directly influence the growth and survival of trees and dictate the accumulation and arrangement of carbon (Adams et al. 2014).

Beyond the well-known climatic and topographic factors important to the distribution of trees (e.g., slope, aspect, and elevation), disturbances are a key process that operate at the landscape scale to change the distribution of forest carbon

storage through the modification of vegetation composition and structure (Thom and Seidl 2016). Therefore, to understand the distributions of carbon stocks at regional scales it is critical to understand the role of disturbance regimes. It is well documented that individual disturbance events have a strong impact on local carbon stocks through either the lateral movement of tree biomass carbon from the standing live pool to the dead pool (Schomakers et al. 2017) or through the removal of tree biomass carbon from the system from combustion or logging practices (North and Hurteau 2011). What is less clear is the impact of disturbance regimes, which are spatially heterogeneous yet may have an impact on carbon accumulation at broad scales. For example, if a disturbance regime is frequent, one would expect lower carbon stocks in areas of higher exposure to that regime (e.g., on steep slopes with frequent avalanches). More fine-scale information on disturbance regimes, climate, and topography might allow for better estimates of the distributions of tree biomass carbon across landscapes. This is especially important in areas that are disproportionally biomass carbon dense (contribute more to global carbon storage than their area would suggest), as changes to those regions can have an

Fig. 1. (a) Map of the perhumid region (dark green) of the coastal temperate North American rainforest (light green on inset map). Points represent the approximate location of permanent sample plots from the Forest Inventory and Analysis dataset in southeast Alaska and Forest Inventory and Analysis Branch dataset in coastal British Columbia. Figure was created using ArcGIS Pro version 2.6.0 with data from the state of Alaska, Esri Canada, and USGS. Coordinate system is Alaska Albers equal area conic, datum WGS 1984, units in meters. We included photos of the overstory (b) and the lower canopy (c) to provide context to readers unfamiliar with this ecosystem. Photos are provided from Trevor Carter.







outsized influence on global carbon cycling (Law et al. 2018, 2023).

One such region is the permanently humid (perhumid) ecoregion of the Pacific Coastal Temperate Rainforest (Fig. 1a; Vynne et al. 2021; DellaSala et al. 2022). Previous research by Buma and Thompson (2019) on the Alaskan coast portion of the perhumid suggests aboveground live tree biomass carbon density will be on average between 225 and 300 Mg C ha⁻¹. Buma and Thompson (2019) also provide expectations on the disturbance regimes for windstorms and landslides, the two primary natural disturbance regimes for the perhumid. It is likely that these two disturbance regimes will have little overlapping area because each regime occurs in unique topographic contexts (e.g., landslides occur on steep slopes). It is unlikely to observe meaningful differences in natural disturbance regimes or historical logging across geopolitical borders in the perhumid (southeast Alaska and coastal British Columbia) because the variability in biogeography and topography is similar across the region. Areas associated with natural disturbance regimes will likely have a slightly higher average aboveground live tree biomass at this spatial scale because these areas are less likely to experience nutrient declines and subsequent biomass loss associated with undisturbed ecosystems (Buma and Thompson 2019), a process sometimes referred to as retrogression (Peltzer et al. 2010). Conversely, the disturbance regime associated with logging, which occurs with a higher frequency than natural disturbances (Krankina et al. 2014), will affect

aboveground live tree biomass. In theory, the effect varies from negative over short timescales (Rhemtulla et al. 2009) to positive over longer timescales as regeneration occurs prior to competitive exclusion of trees (Shugart 1984). However, in practice, logging rotations in the perhumid (e.g., the Tongass NF in southeast Alaska) typically occur on shorter time intervals than what is necessary for forests to reach prelogging conditions (Krankina et al. 2012; Vynne et al. 2021; DellaSala et al. 2022). Understanding the effects of logging on aboveground tree biomass carbon is especially important when considering the future of forest management in this region. The United States has logging policies in the Tongass NF (the northern portion of the perhumid) that focus on (but are not exclusive to) the harvest of younger trees in previously harvested areas (Vilsack 2013) while the management strategies adopted by the Canadian government primarily focus on the conservation of old growth forests (James 2016).

To generate more fine scale estimates of the distribution of aboveground live tree biomass carbon and address the gaps in our understanding of the impacts of disturbance regimes on aboveground live tree biomass carbon, we ask the following questions in the carbon dense perhumid region of the Pacific Coastal Temperate Rainforest of North America: (1) What is the spatial distribution of aboveground live tree biomass carbon across the region? (2) What are the spatial patterns of disturbance regimes across the region? (3) How do disturbance regimes (both natural and anthropogenic) interact across and within geopolitical boundaries to influence aboveground live tree biomass carbon stocks?

Materials and methods

Study region

The perhumid region of the Pacific Coastal Temperate Rainforest is a carbon dense landscape (Leighty et al. 2006; McNicol et al. 2019), which ranges from Yakutat in southeast Alaska through the central coast of British Columbia near Bella Coola (Fig. 1a). The perhumid region of the Pacific Coastal Temperate Rainforest covers 14.7 million ha of land area and 11.6 million ha of forested area (including the Tongass NF and Glacier Bay NP in Alaska and the Great Bear Rainforest in British Columbia as well as private and tribal lands), spanning from sea level to over 2000 m in elevation and extends less than 100 km from the coast (Fig. 1). Mean annual temperature ranges from −14.3 °C in the mountains to 5.6 °C at the southern coast while mean annual precipitation varies from 610 to 5690 mm (Fick and Hijmans 2017). Only a few tree species are dominant in this forest, including Picea sitchensis, Tsuga heterophylla, and to a lesser degree Tsuga mertensiana and Callitropsis nootkatensis. Species such as Pseudotsuga menziesii and Thuja plicata, found further south, extend slightly into the perhumid region but are not major components of the forest. Hardwood species mostly in the genus Alnus and Salix are found in the understory throughout the forest and can dominate scarified soil beds and riparian ar-

Disturbance regimes

This ecosystem is documented to have the lowest frequency of forest disturbances on the North American continent (Buma et al. 2017) with the absence of a definable dry season and a subsequent lack of wildfire as a disturbance process within the last 5000 years (DellaSala 2011). In addition to the lack of historical fire, there is no evidence of substantial insect mortality (Harris 1999). There is a large documented die-off of C. nootkatensis in central and southern portions of the study region associated with decreases in persistent snowpacks and root freezing, while this is a major source of C. nootkatensis mortality, we do not include this mortality presently as the causes and consequences of this mortality are variable and based on multiple climatic signals (Comeau and Daniels 2022). We included natural disturbance regimes via the concept of disturbance exposure (Ager et al. 2012). Disturbance events in this region are exceedingly rare (Buma et al. 2017) and are typically not mapped. Thus, we are primarily concerned about their influence in terms of averages over large spatial extents. We used the methods of Kramer et al. (2001) and Buma and Thompson (2019) to map the dominant disturbance exposure as spatially explicit disturbance regimes (windstorms and landslides, respectively). This method provides a relative probability of a given area being disturbed over long run frequencies and assumes the disturbances are relatively consistent in terms of severity, which

is appropriate for these two regimes in this region (Nowacki and Kramer 1998; Read 2015; Foss et al. 2016).

Contemporary logging practices in the region typically clearcut patches of trees (range from <1 to 5180 ha on private land AK; <1-222 ha on USFS land AK; <1-937 ha in British Columbia) and is a more spatially extensive and more frequent factor compared to natural disturbances (Krankina et al. 2014). We obtained the logging area and year of logging in the region from the US Forest Service and private industry (U.S. Forest Service 2022), and from the BC Ministry of Forests (Forest Analysis and Inventory Branch 2023). The logging data does not define specific harvest practices, although clearcuts are typically standard management practice for this region. We rasterized the logging polygons and created two spatially explicit logging layers (ESRI 2020). The first layer was a binary representation of logging to determine its presence or absence. The second layer represented the time in years since the logging occurred.

Plot data

In southeast Alaska, we used Forest Inventory and Analysis plots (FIA; n = 2315; Gray et al. 2012) and in coastal British Columbia, we used permanent sample plots from the Forest Analysis and Inventory Branch (FAIB; n = 950; Forest Analysis and Inventory Branch 2023). FIA plots are stratified across the landscape (1 plot every 6000 acres) in forested areas and consist of up to four subplots. FAIB plots consist of either fixed or variable radius plots and are stratified along 20 km × 20 km grids. The spatial distribution of permanent sample plots is not even across the study area, with more plots located in southeast Alaska (Fig. 1a). Because multiple observers and years are associated with both the FIA and FIAB data, we validated the logging data reported in these datasets through visual confirmation of logging scars, and to the best of our ability ensured the reported date of logging for each plot matched satellite imagery and other raster layers. Importantly, several plots were reported as being logged and confirmed to have been logged through satellite imagery but contained data (e.g., multiple trees >50 cm Diameter at Breast Height (DBH)) that was unsupportive of an area being logged. As such we removed plots (n = 4) from our analysis that contained biomass values greater than the 80th percentile of live tree biomass and were reported as being logged within the last 20 years, as it is unlikely that regeneration of this scale occurred within 20 years post logging. Additionally, several different plots in coastal British Columbia were reported with the same coordinates and so were removed for our spatially explicit models leading to a final sample size of n = 2218. Lastly, if the same plot was measured on multiple occasions, we used the latest measurement data.

We created area standardized estimates (Mg C ha⁻¹) for each plot using Kozak's allometric equations (Kozak et al. 1969). Kozak's tapering equations, developed for the region, accounts for trees with broken tops and minimizes overestimates of aboveground live tree biomass (Turchick 2021). Given our focus on spatial variation of carbon, the use of additional allometric equations would reproduce the same trends of variation (Turchick 2021). All allometric equations are in-

herently limited to the range of trees upon which they are calibrated. In this region, there are occasionally trees outside any developed allometric system (e.g., >1 m DBH for Tsuga sp.; Table A1). This presents a challenge for unbiased estimations (see discussion), thus we create two estimates that attempt to bracket the true value. We first estimate carbon including all reported tree sizes from the FIA and FAIB data (henceforth the unconstrained estimate). This estimate is potentially biased relative to actual tree biomass carbon (and likely higher, due to the exponential allometric equations), as we are applying the allometric equation to trees beyond the range at which they were calibrated. There is no way to quantify the error associated with estimating tree biomass carbon for trees outside of the range of the equation. We then repeated the same process but truncated trees outside the range of the Kozak equation to be the maximum size within the range of the allometric equation (subsequently referred to as the truncated estimate; Table A1) and report subsequent results in the supplement. This truncated estimate is negatively biased and underrepresents the true level of aboveground live tree biomass carbon as a result. We expect true aboveground live tree biomass carbon is most likely between the two estimates. For both analyses, we grouped estimates of aboveground live tree biomass carbon by plot, year of measurement, and status.

We repeat our analyses a second time for a subset of the data that only includes fixed radius plots. This subset is reported in depth in the supplemental materials and decreases our sample size from n = 2218 to 1852, with all variable radius plots that we excluded being located on the central coast of British Columbia. Due to differences in sampling methodology between fixed radius and variable radius plots, the inclusion of variable radius plots may bias our dataset and their inclusion could lead to decreased model performance. However, we elect to retain all data available for the analyses present in the main text as we view the exclusion of data for the primary purpose of increasing model performance as not best practice.

Machine learning model framework

To estimate regional aboveground live tree biomass carbon and associated prediction intervals in a spatially explicit manner we used quantile regression forests (QRF; Meinshausen 2017). Quantile regression forest is a machine learning framework that operates similar to random forest with the ability to estimate values for any quantile that is needed, which may then be utilized for calculating spatially explicit prediction intervals (e.g., 80%) through using upper (90%) and lower (10%) quantile maps (Koenker and Hallock 2001). We trained a QRF using a randomized training set composed of 80% of the data and an independent test set composed of 20% of the data to produce spatially explicit predictions of aboveground live tree biomass carbon for the 0.1, 0.5, and 0.9 quantiles (Meinshausen 2017).

We included the spatially explicit raster layers of disturbance exposures as predictors as well as elevation, slope, and aspect (LP DAAC 2011), mean annual precipitation and annual temperature (Fick and Hijmans 2017), and percentage

forest cover (Hansen et al. 2013) at a 30 m resolution. Given the inclusion of ice caps and glaciers flowing to low elevations in the study area, we clipped the estimates of aboveground live tree biomass carbon by the forest cover layer to remove estimates of aboveground live tree biomass carbon where no forest cover is present (ESRI 2020).

We evaluated the quantile regression forest model performance using five randomized data folds for cross validation to determine root mean absolute error, variance explained, and mean absolute error. Further, we report the non-spatial distribution of residuals (Fig. A1) and we evaluated the uncertainty estimates by calculating the prediction interval coverage probability (Fig. A2) and mean prediction interval as outlined in Kasraei et al. (2021).

Spatial analysis framework

To quantify the percentage of the landscape exposed to disturbance regimes we calculated the area with high disturbance exposure (arbitrarily set at values greater than the 70th percentile of windstorms or landslides, calculated independently) and logged areas. We then estimated the colocation between disturbance regimes by counting the overlapping areas of modeled disturbance exposure. Additionally, we determined whether areas of disturbance or high disturbance exposure varied topographically and climatically from areas without disturbance or exposure by visually comparing the sampling distributions (mean of 100 random samples repeated 1000 times) for precipitation, slope, and elevation in high and low exposed areas. We utilized t tests to further compare the sampling distributions of high and low exposed areas for these variables. To show the variation in aspect, we randomly sampled aspect 1000 times but did not compute the mean or conduct a t test because of a circular and non-normal distribution of the variable.

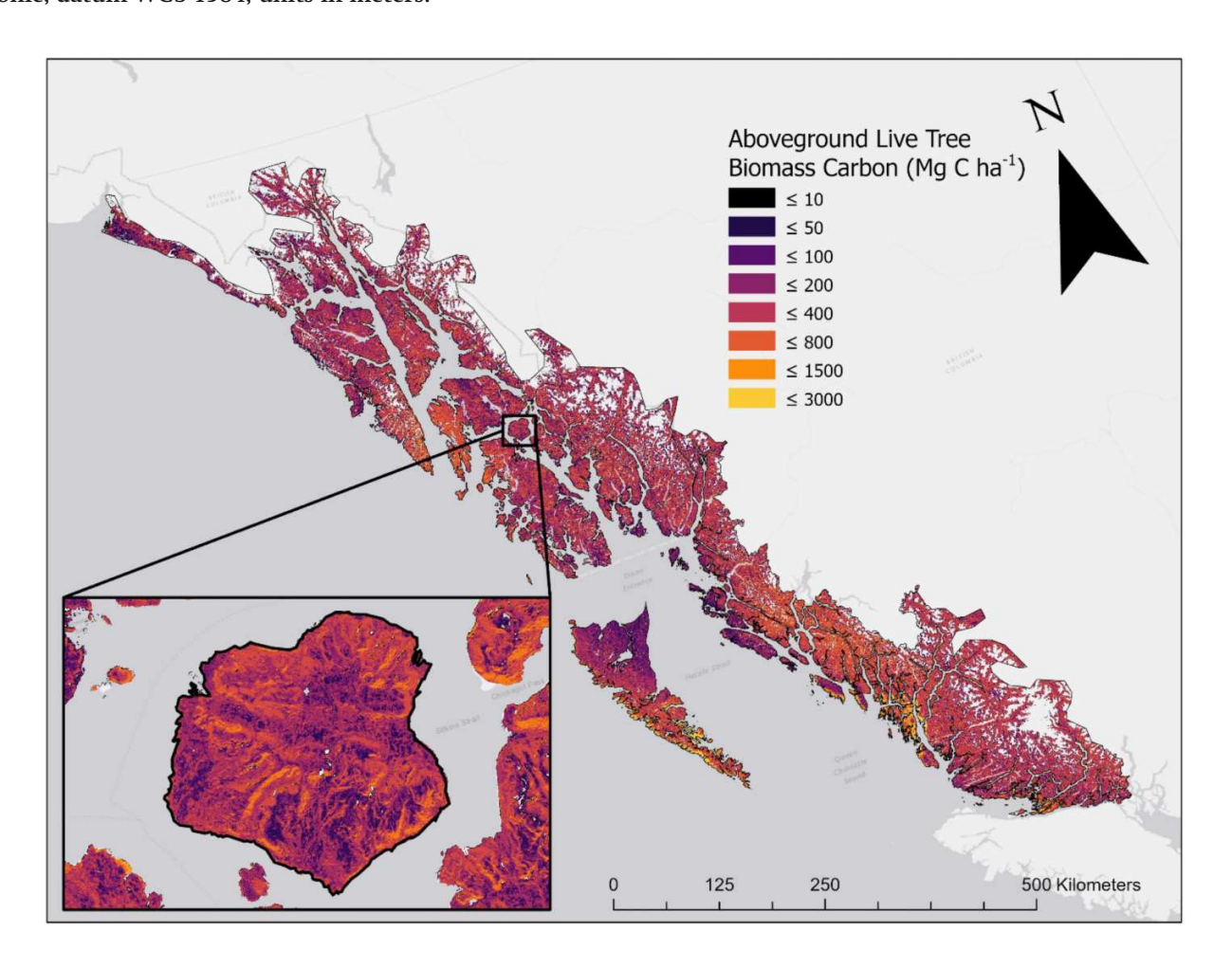
Generalized linear model framework

To address the question of how disturbance types and histories interact to influence aboveground live tree biomass carbon pools, we used a global generalized linear model with a gamma error distribution to identify key statistical correlations using R version 4.1.2 (R Core Team 2022) as follows:

```
Biomass \sim Logged (Y/N) : TimeSinceLogging
         +Logged (Y/N) : TimeSinceLogging<sup>2</sup>
         +Logged (Y/N) \times Country + Wind Regime
         +Landslide Regime + Slope + Precipitation
         + Temperature + Latitude × Longitude
```

We included terms for natural disturbance regimes as represented through disturbance exposure and a binary term for logging to indicate if a plot was measured in a logged area that interacted with another coefficient for time since logging or country of origin (Table A2). The terms for natural disturbance exposure were both continuous variables (ranging from 0 to 1) and are separate from the discrete categories used in the spatial analysis framework. Additionally, we included a polynomial term for time since logging to

Fig. 2. Unconstrained estimate (n = 2218) of aboveground live tree biomass carbon for the perhumid region. Lighter orange and yellow colors indicate more aboveground live tree biomass. The mean aboveground live tree biomass for the region is 218 Mg ha⁻¹ and the maximum predicted aboveground live tree biomass for the region is 2670 Mg ha⁻¹. Figure was created using ArcGIS Pro version 2.6.0 with data from the state of Alaska, Esri Canada, and USGS. Coordinate system is Alaska Albers equal area conic, datum WGS 1984, units in meters.



better understand potential peaks in aboveground live tree biomass that may occur prior to canopy closure (Table A2). We included slope, precipitation, and temperature in our model because both covariates are geographically controlled and may influence aboveground live tree biomass accumulation in this region (Table A2; Buma et al. 2017). We tested our predictors for collinearity using variable influence factors outlined in (Zuur et al. 2009). Finally, we tested our model for residual spatial autocorrelation using the Moran's I statistic. To reduce residual spatial autocorrelation, we included an interaction between latitude and longitude in our model structure. However, this did not completely resolve the residual spatial autocorrelation. As such, we report the residuals as they vary along gradients present in our model (Fig. A3).

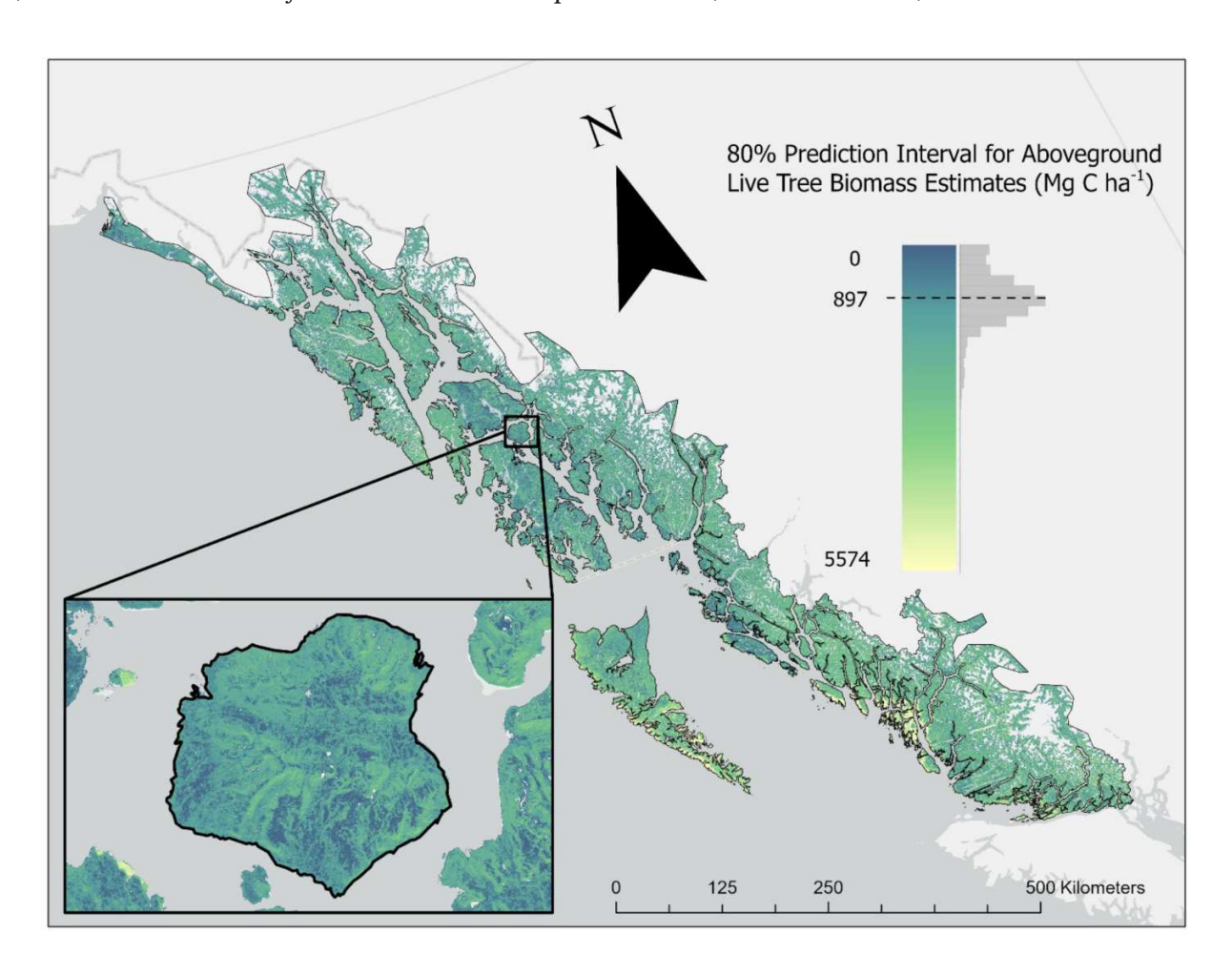
Results

Aboveground tree biomass carbon estimates

Our estimate from the quantile regression forest of aboveground live tree biomass carbon using our unconstrained estimate across the region is comparable to the averages of aboveground live tree biomass within the plot data (predicted $median = 495 \text{ Mg C } ha^{-1} \text{ vs. dataset } median = 478 \text{ Mg C } ha^{-1}).$ Root mean standard error was 520 Mg C ha⁻¹, with mean absolute error of a similar magnitude at 346 Mg C ha⁻¹ and 39% of variance explained. The unconstrained estimate of median predicted aboveground live tree biomass carbon ranges from 5 Mg C ha⁻¹ in sparsely forested areas (e.g., higher elevations or muskeg environments) to 2670 Mg C ha^{-1} and was on average 218 Mg C ha^{-1} (SD = 169 Mg C ha^{-1} ; Fig. 2). Total regional aboveground live tree biomass carbon for our unconstrained estimate was 2.5 Pg of carbon. The 80% prediction interval was on average 1140 Mg C ha⁻¹ with 77% of predictions from the model falling within the prediction interval and 81% of prediction intervals containing the value of aboveground live tree biomass estimated from the FIA and FAIB dataset (Figs. 3 and A2).

The quantile regression forest model for the truncated estimate performed similarly to the model using the unconstrained estimate, with a root mean standard error of 461 Mg C ha⁻¹, a mean absolute error of 319 Mg C ha⁻¹, and 43% of the variance explained. The model for the truncated estimates

Fig. 3. The spatially explicit 80% prediction interval for the unconstrained estimate of aboveground live tree biomass carbon (Mg C $\rm ha^{-1}$). The prediction interval coverage probability is 80.57% while 76.91% of predictions are within the prediction interval. The mean prediction interval (non-shown on histogram) was 1140 Mg C $\rm ha^{-1}$, while median prediction interval (shown with dashed line) was 897 Mg C $\rm ha^{-1}$. Figure was created using ArcGIS Pro version 2.6.0 with data from the state of Alaska, Esri Canada, and USGS. Coordinate system is Alaska Albers equal area conic, datum WGS 1984, units in meters.



mate predicted a slightly smaller average than the model for the unconstrained estimate, with 211 Mg C ha^{-1} (SD = 163 Mg C ha⁻¹) being stored as aboveground live tree biomass (Fig. A4). This estimate set is on average 7 Mg C ha^{-1} (3%) lower than the unconstrained estimate of aboveground live tree biomass carbon (Fig. A5). The truncated estimate of predicted aboveground live tree biomass carbon is also comparable although slightly higher than averages of aboveground live tree biomass carbon within the dataset of permanent sample plots (predicted median = $472 \text{ Mg C ha}^{-1} \text{ vs. dataset}$ $median = 469 \text{ Mg C } ha^{-1}$). Our truncated estimate of median aboveground live tree biomass carbon ranges from 5 to 2620 Mg C ha⁻¹ in forested areas and is in total 2.3 Pg of carbon. The 80% prediction interval for the quantile regression forest model using the truncated estimate of aboveground live tree biomass was on average 1061 Mg C ha⁻¹ with 77% of predictions from the model being contained within the prediction interval and 80% of the prediction intervals containing the value of aboveground live tree biomass estimated from the FIA and FAIB dataset (Fig. A6).

Disturbance regimes across the forest

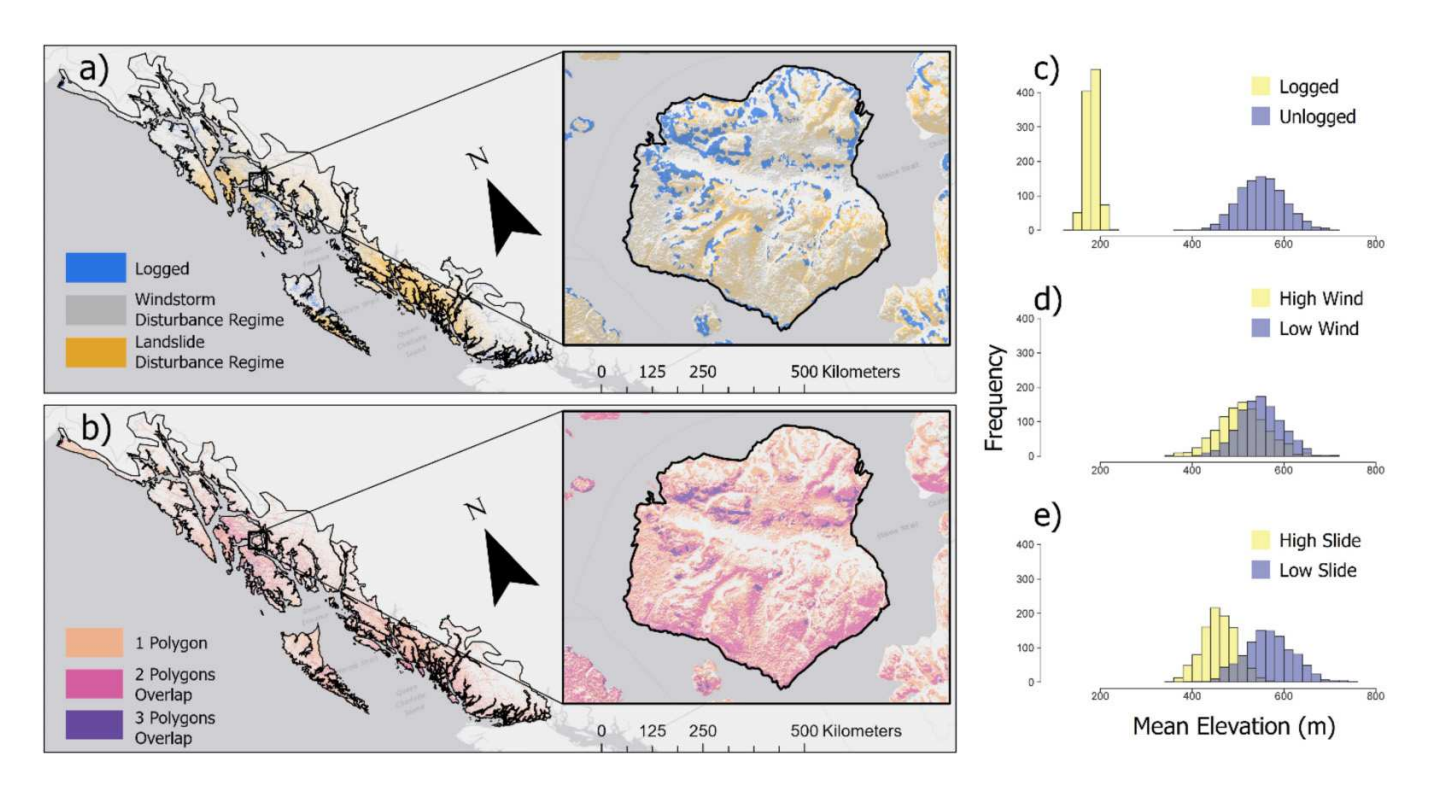
Logging affected approximately 6% of forested area (data from 1945 to 2014) in the perhumid region with each country having comparable forested area logged (Table 1; Fig. 4a). Similarly, disturbance regimes (not individual disturbance events) for both landslides and windstorms in southeast Alaska and coastal British Columbia associated with similar amounts of forested area (Table 1; Fig. 4a). Over half of the forest area (69.5%; approx. 8 million ha; Table A3) was associated with the conditions that align with a natural disturbance regime or experienced logging (Fig. 4b). Within this approximately 8 million ha, 38.2% of the land area was logged or aligned with one natural disturbance regime (landslides or windstorms), 29.0% of land area had environmental conditions that accompany both natural disturbance regimes, or had conditions associated with one disturbance regime and was logged. Less of the landscape (2.21%) experienced logging and was associated with the disturbance regimes for both natural disturbances. There is no major bias of overlapping logging and disturbance regimes based on geopolitical boundary

Table 1. Summary of the area logged (time range 1945–2014) or associated with natural disturbance regimes (modelled) for southeast Alaska, coastal British Columbia and in total (AK + BC).

Disturbance	Area of disturbance (ha)	Area of forest (ha)	Area (%)
Logging AK	305 000	6 110 000	4.99%
Logging BC	381 000	5 490 000	6.95%
Logging total	687 000	11 600 000	5.92%
Wind regime AK	1 840 000	6 110 000	30.1%
Wind regime BC	1 750 000	5 490 000	31.9%
Wind regime total	3 590 000	11 600 000	30.9%
Landslide regime AK	1 540 000	6 110 000	25.2%
Landslide regime BC	2240000	5 490 000	40.9%
Landslide regime total	3 780 000	11 600 000	32.6%

Note: Area is reported both in hectares and as a percentage of forested area in relation to southeast Alaska (6.11 million ha), costal British Columbia (5.49 million ha), and the perhumid region (11.6 million ha). Logged areas vary in time since logging (span of 67 years) but are reported as such in either the FIA or FIAB dataset. Area for natural disturbance regimes are >70th percentile of relative frequency for each respective natural disturbance (for full description see methods).

Fig. 4. (*a*) Map of the area that either experienced logging or was associated with the conditions that align with the disturbance regimes (i.e., exposure) of windstorms or landslides. (*b*) The number of overlapping polygons from panel (*a*). Figure was created using ArcGIS Pro version 2.6.0 with data from the state of Alaska, Esri Canada, and USGS. Coordinate system is Alaska Albers equal area conic, datum WGS 1984, units in meters. Variation in the sampling distribution for the mean of elevation for (*c*) logged and unlogged areas, (*d*) high and low relative frequency for the windstorm disturbance regime, and (*d*) high and low relative frequency for the landslide disturbance regime. High and low relative frequencies of disturbance regimes (disturbance exposure) are greater than or equal to the 70th percentile and lower than the 70th percentile of relative disturbance frequency respectively.



(Table A3), this is result is not sensitive to the arbitrary cutoff used to define high versus low disturbance regimes.

Logged areas were biased towards areas with higher mean precipitation, lower slopes, and lower elevations (Fig. 4c) but did not vary with regards to aspect (Fig. A7c). Logging did

not disproportionately occur in areas with natural disturbance regimes (Fig. A8). Unsurprisingly, the presence of logging was correlated with significantly lower aboveground live tree biomass carbon (Table 2; Fig. A9). Predicted aboveground live tree biomass carbon was slightly higher in un-

Table 2. Model results estimating the effect of the relative frequency of natural disturbance regimes and logging across geopolitical borders on aboveground live tree biomass carbon using the unconstrained estimate of plots (n = 2218).

Biomass \sim Disturbance regimes $+$ Slope $+$ Precipitation $+$ Temperature $+$ Latitude \times Longitude $(N=2218)$ — $R^2=0.238$				
Coefficient	Estimate	SE (Standard Error)	t-value	P-value
Unlogged	-22.4	19.2	- 1.16	0.245
Logged	-4.03	0.450	-8.96	< 0.001
BC unlogged	1.22	0.107	11.4	< 0.001
BC logged	-1.18	0.160	-7.33	< 0.001
Wind regime	0.002	0.010	0.193	0.847
Landslide regime	-0.240	0.499	-0.480	0.631
Precipitation	0.001	0.000	1.23	0.217
Temperature	0.068	0.015	4.51	< 0.001
Slope	0.021	0.003	6.83	< 0.001
Logged (Y) × TimeSince	0.110	0.027	4.00	< 0.001
Logged (Y) \times TimeSince ²	-0.001	0.000	-1.54	0.123
Latitude	0.634	0.351	1.81	0.071
Longitude	-0.130	0.151	-0.857	0.391

Note: Covariates for slope and precipitation are included to further elucidate the effect of landslides

0.003

logged forests in coastal British Columbia and slightly lower in logged forests in coastal British Columbia as compared to unlogged and logged forests in southeast Alaska, respectively (Table 2; Fig. A9). On average, unlogged plots in southeast Alaska had $461 \pm 22 \text{ Mg C ha}^{-1}$ while logged plots in southeast Alaska had 189 \pm 49 Mg C ha $^{-1}$ and unlogged plots in coastal BC had 1047 ± 59 Mg C ha⁻¹ with logged plots having 160 \pm 47 Mg C ha $^{-1}$ (mean \pm 95% CI). In logged areas, the effect of the time since logging (over a span of 67 years) had a significant linear effect on aboveground live tree biomass carbon such that with increasing time since logging aboveground live tree biomass was higher than areas with less time since logging (Fig. A10). Plots associated with the lowest time since logging (1 year) were associated with $7.0 \pm 6.3 \,\mathrm{Mg}\,\mathrm{C}\,\mathrm{ha}^{-1}$ while plots associated with the highest time since logging (67 years) were associated with 579 \pm 484 Mg C ha⁻¹ (mean \pm 95% CI), with the confidence around the mean decreasing with increasing time since logging (Fig. A10). We did not observe a decrease in estimated aboveground live tree biomass associated with the quadratic term for time since logging.

Latitude × Longitude

Areas with high exposure to windstorm disturbance regimes are biased towards comparatively less steep slopes, southwesterly aspects, and to a lesser degree lower elevations than areas with low exposure to windstorm disturbance regimes (Figs. 4d and A7). Areas with high exposure to landslide disturbance regimes differed meaningfully from areas with low exposure in all topographic contexts tested. Specifically, areas with high exposure to landslide disturbance regimes had higher mean precipitation, steeper slopes, more southern aspects, and lower elevations (Fig. 4e and A7). Areas with a high exposure to one disturbance regime were positively associated with areas with a high exposure to the other disturbance regime (i.e., areas of high landslide exposure were also in areas of high windstorm exposure

and vice-versa; Figs. 4 and A8). Overall, natural disturbance regimes were not important predictors of aboveground live tree biomass carbon for the region (Table 2). Slope significantly predicted aboveground live tree biomass carbon such that steeper slopes on average had higher aboveground live tree biomass carbon.

0.219

Discussion

0.003

Aboveground tree biomass carbon

Our study represents the most detailed investigation of spatially explicit aboveground live tree biomass carbon distributions in the perhumid region of the Pacific Coastal Temperate Rainforest to date. Our median estimates of aboveground live tree biomass carbon ranged between 2.3 and 2.5 Pg of carbon (Figs. 2 and A4). We estimate this forest has on average either 211 Mg C ha^{-1} (SD = 163 Mg C ha^{-1}) or 218 Mg C ha^{-1} (SD = 169 Mg C ha^{-1}) stored in aboveground live tree biomass. Our estimates largely align with previous spatially explicit estimates of tree biomass carbon densities for southeast Alaska (1.21-1.52 Pg C: Buma and Thompson 2019), and are slightly higher than previous estimates that do not employ spatially explicit estimation methods (0.45 Pg C: Law et al. 2023; 0.42-0.53 Pg C: Leighty et al. 2006). Our estimates are also comparable with other high-end carbon density estimates of globally important and highly productive forests (Santoro et al. 2021). The perhumid region disproportionally contributes to global forest carbon storage; the perhumid region consists of approximately 0.3% of global forest area (Pan et al. 2011; Keenan et al. 2015) but the data here suggest that it stores between 0.63% and 1.07% of global aboveground forest carbon as aboveground live tree biomass (Kindermann et al. 2008; Pan et al. 2011; Santoro et al. 2021).

Patterns of disturbance regimes

Disturbance regimes did have distinct spatial patterns, both individually (Fig. 4) and relative to each other (Fig. A8). Logging did not preferentially occur on areas with high exposure to landslide or windstorm regimes. However, natural disturbance regimes were co-located despite different trends in the topographic and climatic positioning of mean sampling distributions for each respective disturbance regime (Table A3; Fig. A7). Although we did not observe a bias of logged sites occurring in areas of more frequent natural disturbances at this spatial scale, there are many similarities in the topographic positioning between logging and natural disturbance regimes. Both logging and landslides are biased towards areas of higher precipitation and lower elevations, while logging and windstorms tend to occur on lower slopes. Notably, the means of each disturbance or disturbance regimes have minor differences for each topographic

Surprisingly, we did not observe any trends of natural disturbance regimes on aboveground live tree biomass carbon storage, as was observed in Buma and Thompson (2019). The lack of effect may be in part because natural disturbances are infrequent in absolute terms across this landscape (Buma et al. 2017), or because disturbance events lack the magnitude to impact biomass carbon accumulation at this scale (Turchick 2021). While our sample area only comprises less than 1% of the landscape, the failure to detect an effect of natural disturbance regimes on aboveground live tree biomass is likely not due to an inadequate sample size. Our sample, albeit not spatially random, is representative of the population we are modelling. A post hoc power analysis provides evidence that our sample size was sufficient to detect an effect as small as 0.08 (df = 2204, n = 2218, $\alpha = 0.05$). In contrast, logging decreased aboveground live tree biomass carbon (Table 2) and the effect of time since logging showed a positive relationship with aboveground live tree biomass carbon (Fig. A10).

Influence of logging

Unsurprisingly, logging decreased aboveground live tree biomass, which is intuitive and well documented in other systems (Mathys et al. 2013; DellaSala et al. 2022). The effect of logging typically differs from natural disturbance regimes, as carbon is removed from the landscape as compared to transferred laterally from one pool to another. The effect of logging on aboveground live tree biomass carbon was consistent across geopolitical borders, although the magnitude of the effect varied slightly by country (Fig. A9). The positive relationship of time since logging with aboveground live tree biomass carbon aligns with biomass accumulation during stand regeneration. The variation in operational-level practices (e.g., slash and logging debris left on site, non clearcut operations, etc.) may also result in the high variability observed within logged plots, though we did not have data to detect that actor. We note that the dataset is limited in temporal coverage, going back to the 1950s. It is possible that inadequate representation of older logging locations precluded capturing further changes in aboveground live tree biomass as stand

structure closes in our model (Shugart 1984). The effect of logging is especially important when considering the future of forest management in this region. The United States has recently adopted new logging policies that primarily focus on the harvest of younger trees exclusive to the Tongass NF portion of the study region (Vilsack 2013). This contrasts with the management strategies adopted by the Canadian government, which focus on conservation and has taken land out of the harvest rotation, although some logging does still occur (James 2016). Policy focused on re-logging areas will continue to disturb highly productive areas (i.e., valley bottoms) that might serve as aboveground live tree biomass carbon refuges. The continued effect of logging, if done in the same locations, may not result in large changes to carbon storage in the landscape unless intensified, but that also implies a regional carbon level lower than potential carbon stocks were logging activity to be shifted or reduced (Leighty et al. 2006; DellaSala et al. 2022). We observed a slight but noticeable trend of aboveground live tree biomass increasing with time since logging. This trend is underscored by the high variance in aboveground live tree biomass carbon in plots that experienced logging. The conservation of coastal British Columbia forests is particularly important because of their slight but significantly higher levels of aboveground live tree biomass carbon as compared to southeast Alaska.

Limitations and challenges

The models selected, which incorporate disturbance regimes, while appropriate for our understanding at broad spatial scales, are not intended to understand individual disturbance events nor processes at finer spatial scales. We are not aware of any dataset for natural disturbances that span the entire study region at a temporal scale that would be appropriate to address questions of aboveground live tree biomass carbon storage. Mapping at regional scales requires subsuming heterogeneous local factors and local data set limitations, which may be significant at local scales, into broader modeling frameworks. For example, the data available in both southeast Alaska and coastal BC for logging do not represent a complete history of logging in the region; however, at broad spatial scales our data represents similar trends to the landscape (approx. 6% of plots experienced logging and approx. 6% of landscape experienced logging). To help address uncertainty in data, we included a variety of estimates of aboveground live tree biomass carbon (see supplemental materials) and expressly caution against using a singular estimate for management and policy decisions. The prediction intervals were on average large in both the unconstrained estimate set (1140 Mg C ha⁻¹; Fig. 3) and truncated estimate set (1061 Mg C ha⁻¹; Fig. A6). The variation that we observed within each estimate set is likely because of the variation present within the data collected across a broad geographic area (see Fig. 1a), which was propagated by the quantile regression forest throughout its estimating procedures (supplemental materials). The disparity of plot number and continuity between the United States and Canada is likely causing some of the spatial autocorrelation, as there are spatial gaps between the two efforts and additional sampling efforts will likely decrease the variance present in the models.

There are also challenges associated with allometric equations, which were developed for trees ranging from 12.7 to 215.9 cm DBH in the Pacific Coastal Temperate Rainforest (Table A1). The largest trees hold a disproportionate amount of tree biomass carbon. This makes it impossible to properly estimate uncertainty for the full dataset, because the sizes of some trees are outside the range of tree sizes used to develop the Kozak tapering equation (or any allometric for these species). We suggest the unconstrained estimate is likely closer to the true value, because it includes the full range of tree sizes, but it is impossible to fully quantify the error. Conversely, our truncated estimate, which does not fully account for these trees is certainly an underestimate of true tree biomass carbon but does provide a strong estimate for the lower range of potential values. Given the growing significance of carbon storehouses in global climate accounting (Keith et al. 2014), it is a challenge that must be met by the mensuration community.

Conclusions

The Pacific Coastal Temperate Rainforest is exceptionally carbon dense. Despite multiple spatially explicit predictions of aboveground tree biomass carbon, each estimate needs to be interpreted with caution due to the limitations of quantifying the uncertainty of allometric equations and bias in the spatial coverage of plots. Aboveground live tree biomass carbon is relatively insensitive to natural disturbance regimes at broad scales; rather, carbon is more strongly associated with topography and climate. Logging is also a strong influence even at regional scales. Logging is far more frequent than natural disturbances on this landscape, and the negative effect of logging on tree biomass carbon storage will persist if forest management plans focus on the harvest of younger trees. Future management plans for the perhumid, which include the Tongass NF and Great Bear Rainforest, should fully consider the impact of harvest on tree biomass carbon storage and how harvest rotations align (or do not align) to the natural disturbance regime as outlined here. This work can inform regional carbon management pracices, which in turn can inform international goals to conserve reservoirs of carbon, such as forests, outlined in the Paris Climate Agreement (article 5) that was signed by both the United States and Canada. The regional map of current aboveground live tree carbon stocks is a useful dataset for planning management activities that could mimic patterns of carbon stocks or natural disturbances at regional scales.

Acknowledgements

We collectively thank Tom Thompson at the US Forest Service and Sari Saunders, Caren Dymond, and Rene De Jong at the British Columbia Ministry of Forests for providing and clarifying data. We would also like to thank two anonymous reviewers for their thoughtful and constructive reviews, Audrey Pearson, Melissa Lucash, James Lamping, Kate Hayes, Erin Twaddell, Rob Scheller, Brian Kleinhenz, Allison Bid-

lack, Suzanne Tank, Ian Giesbrecht, Bill Floyd, Gavin McNicol, Jared Ceplo, Anthony Stewart, Eran Hood, and Megan Behnke.

Article information

History dates

Received: 24 January 2024 Accepted: 17 April 2024

Accepted manuscript online: 19 April 2024 Version of record online: 7 August 2024

Copyright

© 2024 The Author(s). This work is licensed under a Creative Commons Attribution 4.0 International License (CC BY 4.0), which permits unrestricted use, distribution, and reproduction in any medium, provided the original author(s) and source are credited.

Data availability

Forest Inventory and Analysis data and Forest Analysis and Inventory Data are available publicly. However, exact GPS locations for the FIA that are needed to properly reproduce the analysis necessitate a Memorandum of Understanding with the US Forest Service. Corresponding code, spatially explicit topographic, climatic, and disturbance regime raster layers as well as all unconstrained and truncated estimate raster layers are available on Dryad (DOI: 10.5061/dryad. 3tx95x6nn).

Author information

Author ORCIDs

Trevor A. Carter https://orcid.org/0000-0002-8727-5327

Author contributions

Conceptualization: BB
Data curation: TAC, BB
Formal analysis: TAC
Funding acquisition: BB
Investigation: TAC
Methodology: TAC

Project administration: BB

Resources: BB Supervision: BB Validation: TAC Visualization: TAC

Writing – original draft: TAC Writing – review & editing: TAC, BB

Competing interests

The authors declare that they have no known competing financial interests or personal relationships that could have appeared to influence the work reported in this paper.

Funding information

This work was supported by the National Science Foundation (grant number 2025726).

Supplementary material

Supplementary data are available with the article at https://doi.org/10.1139/cjfr-2024-0015.

References

- Adams, H.R., Barnard, H.R., and Loomis, A.K. 2014. Topography alters tree growth-climate relationships in a semi-arid forested catchment. Ecosphere, 5: 1–16. doi:10.1890/ES14-00296.1.
- Ager, A.A., Vaillant, N.M., Finney, M.A., and Preisler, H.K. 2012. Analyzing wildfire exposure and source–sink relationships on a fire prone forest landscape. For. Ecol. Manag. 267: 271–283. doi:10.1016/j.foreco.2011. 11.021.
- Buma, B., and Thompson, T. 2019. Long-term exposure to more frequent disturbances increases baseline carbon in some ecosystems: mapping and quantifying the disturbance frequency-ecosystem C relationship. PLoS One, 14: 1–16. doi:10.1371/journal.pone.0212526.
- Buma, B., Costanza, J.K., and Riitters, K. 2017. Determining the size of a complete disturbance landscape: multi-scale, continental analysis of forest change. Environ. Monit. Assess. 189. doi:10.1007/ s10661-017-6364-x. PMID: 29164343.
- Comeau, V.M., and Daniels, L.D. 2022. Multiple divergent patterns in yellow-cedar growth driven by anthropogenic climate change. Clim. Change, **170**: 22. doi:10.1007/s10584-021-03264-0.
- DellaSala, D.A. 2011. Temperate and boreal rainforests of the world. Island Press.
- DellaSala, D.A., Gorelik, S.R., and Walker, W.S. 2022. The Tongass National Forest, Southeast Alaska, USA: a natural climate solution of global significance. Land, Vol. 11. p. 717. doi:10.3390/land11050717.
 ESRI. 2020. ArcGIS Pro.
- Fick, S.E., and Hijmans, R.J. 2017. WorldClim2: new 1 km spatial resolution climate surfaces for global land areas.
- Forest Analysis and Inventory Branch. 2023. Forest inventory ground plot data and interactive map.
- Foss, J.V, Landwehr, D.J., Silkworth, D., Krosse, P., and Baichtal, J. 2016. Landtype associations of the Tongass National Forest.
- Gray, A.N., Brandeis, T.J., Shaw, J.D., McWilliams, W.H., and Miles, P. 2012.
 Forest Inventory and Analysis Database of the United States of America (FIA). *In* Vegetation databases for the 21st century. Vol. 4. *Edited by*J. Dengler, J. Oldeland, F. Jansen, M. Chytry, J. Ewald, M. Finckh,
 F. Glockler, G. Lopez-Gonzalez, R.K. Peet and J.H.J. Schaminee. pp. 225–231
- Hansen, M.C., Potapov, P.V., Moore, R., Hancher, M., Turubanova, S.A., Tyukavina, A., et al. 2013. High-resolution global maps of 21st-century forest cover change.
- Harris, A.S. 1999. Wind in the forests of southeast Alaska and guides for reducing damage (General Technical Report No. 244), United States Forest Service General Technical Report PNW-GTR_244. USDA Forest Service, Pacific North West.
- James, C. 2016. 2016: Great Bear Rainforest (Forest Management) Act, Bill 2. Legislative Assembly of British Columbia, Victoria, British Columbia.
- Kasraei, B., Heung, B., Saurette, D.D., Schmidt, M.G., Bulmer, C.E., and Bethel, W. 2021. Quantile regression as a generic approach for estimating uncertainty of digital soil maps produced from machinelearning. Environ. Model. Softw. 144: 105139. doi:10.1016/j.envsoft. 2021.105139.
- Keenan, R.J., Reams, G.A., Achard, F., de Freitas, J.V., Grainger, A., and Lindquist, E. 2015. Dynamics of global forest area: results from the FAO Global Forest Resources Assessment 2015. For. Ecol. Manage. 352: 9–20. doi:10.1016/j.foreco.2015.06.014.
- Keith, H., Lindenmayer, D., Mackey, B., Blair, D., Carter, L., McBurney, L. et al. 2014. Managing temperate forests for carbon storage: impacts of logging versus forest protection on carbon stocks. Ecosphere 5(6): 75. doi:10.1890/ES14-00051.1.
- Kindermann, G.E., McCallum, I., Fritz, S., and Obersteiner, M. 2008. A global forest growing stock, biomass and carbon map based on FAO statistics. Silva Fenn. 42: 387–396. doi:10.14214/sf.244.
- Koenker, R., and Hallock, K.F. 2001. Quantile regression.

- Kozak, A., Munro, D.D., and Smith, J.H.G. 1969. Taper functions and their application in forest inventory. For. Chron. 45: 278–283. doi:10.5558/ tfc45278-4.
- Kramer, M.G., Hansen, A.J., Taper, M.L., and Kissinger, E.J. 2001. Abiotic controls on long-term windthrow disturbance and temperate rain forest dynamics in Southeast Alaska. Ecology, 82: 2749–2768. doi:10.1890/0012-9658(2001)082%5b2749:ACOLTW%5d2.0.CO;2.
- Krankina, O.N., DellaSala, D.A., Leonard, J., and Yatskov, M. 2014. High-biomass forests of the Pacific Northwest: who manages them and how much is protected? Environ. Manage. 54: 112–121. doi:10.1007/s00267-014-0283-1. PMID: 24894007.
- Krankina, O.N., Harmon, M.E., Schnekenburger, F., and Sierra, C.A. 2012. Carbon balance on federal forest lands of Western Oregon and Washington: the impact of the Northwest Forest Plan. For. Ecol. Manage. **286**: 171–182. doi:10.1016/j.foreco.2012.08.028.
- Law, B.E., Berner, L.T., Wolf, C., Ripple, W.J., Trammell, E.J., and Birdsey, R.A. 2023. Southern Alaska's forest landscape integrity, habitat, and carbon are critical for meeting climate and conservation goals. AGU Adv. 4: e2023AV000965. doi:10.1029/2023AV000965.
- Law, B.E., Hudiburg, T.W., Berner, L.T., Kent, J.J., Buotte, P.C., and Harmon, M.E. 2018. Land use strategies to mitigate climate change in carbon dense temperate forests. Proc. Natl. Acad. Sci. U.S.A. 115: 3663–3668. doi:10.1073/pnas.1720064115. PMID: 29555758.
- Leighty, W.W., Hamburg, S.P., and Caouette, J. 2006. Effects of management on carbon sequestration in forest biomass in southeast Alaska. Ecosystems, 9: 1051–1065. doi:10.1007/s10021-005-0028-3.
- Litton, C.M., Raich, J.W., and Ryan, M.G. 2007. Carbon allocation in forest ecosystems. Global Change Biol. 13: 2089–2109. doi:10.1111/j. 1365-2486.2007.01420.x.
- LP DAAC (NASA Land Processes Distributed Active Archive Center) 2011. ASTER GDEM2. USGS/Earth Resources Observation and Science (EROS) Center, Sioux Falls, South Dakota [accessed August 2018].
- Mathys, A., Black, T.A., Nesic, Z., Nishio, G., Brown, M., Spittlehouse, D.L., et al. 2013. Carbon balance of a partially harvested mixed conifer forest following mountain pine beetle attack and its comparison to a clear-cut. Biogeosciences, **10**: 5451–5463. doi:10.5194/bg-10-5451-2013.
- McNicol, G., Bulmer, C., D'Amore, D., Sanborn, P., Saunders, S., Giesbrecht, I., et al. 2019. Large, climate-sensative soil carbon stocks mapped with pedology-informed machine larning in the North Pacific Coastal Temperate Rainforest. Environ. Res. Lett. 27: 0–31. doi:10.1080/14484846.2018.1432089.
- Meinshausen, N. 2017. quantregForest.
- North, M.P., and Hurteau, M.D. 2011. High-severity wildfire effects on carbon stocks and emissions in fuels treated and untreated forest. For. Ecol. Manage. 261: 1115–1120. doi:10.1016/j.foreco.2010.12.039.
- Nowacki, G.J., and Kramer, M.G. 1998. The effects of wind disturbance on temperate rain forest structure and dynamics of southeast Alaska. USDA Forest Service—General Technical Report PNW.
- Pan, Y., Birdsey, R.A., Fang, J., Houghton, R., Kauppi, P.E., Kurz, W.A., et al. 2011. A large and persistent carbon sink in the world's forests. Science, 333. doi:10.1126/science.1201609. PMID: 21764754.
- Peltzer, D.A., Wardle, D.A., Allison, V.J., Baisden, W.T., Bardgett, R.D., Chadwick, O.A., et al. 2010. Understanding ecosystem retrogression. Ecol. Monogr. 80: 509–529. doi:10.1890/09-1552.1.
- R Core Team. 2022. R: a language and environment for statistical computing.
- Read, W.A. 2015. The climatology and meteorology of windstorms that affect southwest British Columbia, Canada, and associated tree-related damage to the power distribution grid.
- Rhemtulla, J.M., Mladenoff, D.J., and Clayton, M.K. 2009. Historical forest baselines reveal potential for continued carbon sequestration. Proc. Natl. Acad. Sci. U.S.A. 106: 6082–6087. doi:10.1073/pnas.0810076106. PMID: 19369213.
- Santoro, M., Cartus, O., Carvalhais, N., Rozendaal, D.M.A., Avitabile, V., Araza, A., et al. 2021. The global forest above-ground biomass pool for 2010 estimated from high-resolution satellite observations. Earth Syst. Sci. Data, 13: 3927–3950. doi:10.5194/essd-13-3927-2021.
- Schomakers, J., Jien, S.-H., Lee, T.-Y., Huang, J.-C., Hseu, Z.-Y., Lin, Z.L., et al. 2017. Soil and biomass carbon re-accumulation after landslide disturbances. Geomorphology, 288: 164–174. doi:10.1016/j.geomorph. 2017.03.032. PMID: 31293283.

Shugart, H.H. 1984. A theory of forest dynamics: the ecological implications of forest succession models. Springer-Verlag.

Thom, D., and Seidl, R. 2016. Natural disturbance impacts on ecosystem services and biodiversity in temperate and boreal forests. Biol. Rev. Cambridge Philos. Soc. **91**: 760–781. doi:10.1111/brv.12193. PMID: 26010526.

 $\label{thm:condition} Turchick, K.R.\ 2021. \ Long\ term\ effects\ of\ disturbance\ processes\ on\ ecosystem\ properties.$

U.S. Forest Service. 2022. S_USA.Activity_TimberHarvest.

Vilsack, T. 2013. Addressing sustainable forestry in southeast Alaska.

Vynne, C., Dovichin, E., Fresco, N., Dawson, N., Joshi, A., Law, B.E., et al. 2021. The importance of Alaska for climate stabilization, resilience, and biodiversity conservation. Front. For. Glob. Change 4: 701277. doi:10.3389/ffgc.2021.701277.

Zuur, A., Ieno, E., Walker, N., Saveliev, A., and Smith, G.M. 2009. Mixed effects models and extensions in ecology with R. Springer Science & Business Media.

Appendix A

Table A1. Species and associated ranges of values for diameter at breast height (DBH) and height used by Kozak (1969) to develop the allometric equation used.

Species	DBH min (cm)	DBH max (cm)	Height min (m)	Height max (m)
Abies amabilis	12.70	60.96	8.53	35.96
Abies lasiocarpa	12.70	60.96	8.53	35.96
Alnus rubra	12.70	45.72	16.15	32.92
Betula papyrifera	12.70	53.34	13.72	27.13
Chamaecyparis nootkatensis	15.24	111.76	13.41	45.11
Picea engelmannii	12.70	66.04	11.28	41.76
Picea glauca	12.70	66.04	11.28	41.76
Picea sitchensis	15.24	215.90	14.63	74.98
Pinus contorta	12.70	58.42	12.80	39.62
Pinus monticola	15.24	68.58	13.72	44.80
Populus balsamifera	12.70	121.92	13.72	50.90
Populus tremuloides	12.70	53.34	12.80	31.39
Pseudotsuga menziesii	12.70	180.34	15.85	70.41
Thuja plicata	15.24	129.54	9.45	57.60
Tsuga heterophylla	12.70	106.68	12.19	53.64
Tsuga mertensiana	12.70	106.68	12.19	53.64

Table A2. Topographic, climatic, and disturbance regime covariates included in the generalized linear model framework (n = 2218).

Covariate	Mean	Standard deviation	Units
Annual mean temperature	-0.384	2.81	Degrees
Annual precipitation	284	85.7	Decimeter
Slope	16.0	10.6	Degrees
Elevation	246	226	Meters
Tree cover	83.3	19.9	Percent
Windstorm regime	0.410	0.232	Relative Probability
Landslide regime	0.100	0.093	Relative Probability
Presence/absence logging	6.40	1351 AK, 867 BC	Percent/# of plots
Time since logging	33.5	12.2	Years

Note: We report mean, standard deviation, and associated units for each variable. For the presence/absence of logging we report what proportion of plots was reported as being logged and the number of plots within each country in place of a standard deviation.

Fig. A1. The nonspatial distribution of residuals for quantile regression forest estimate of the unconstrained estimate of tree biomass carbon (n = 2218).

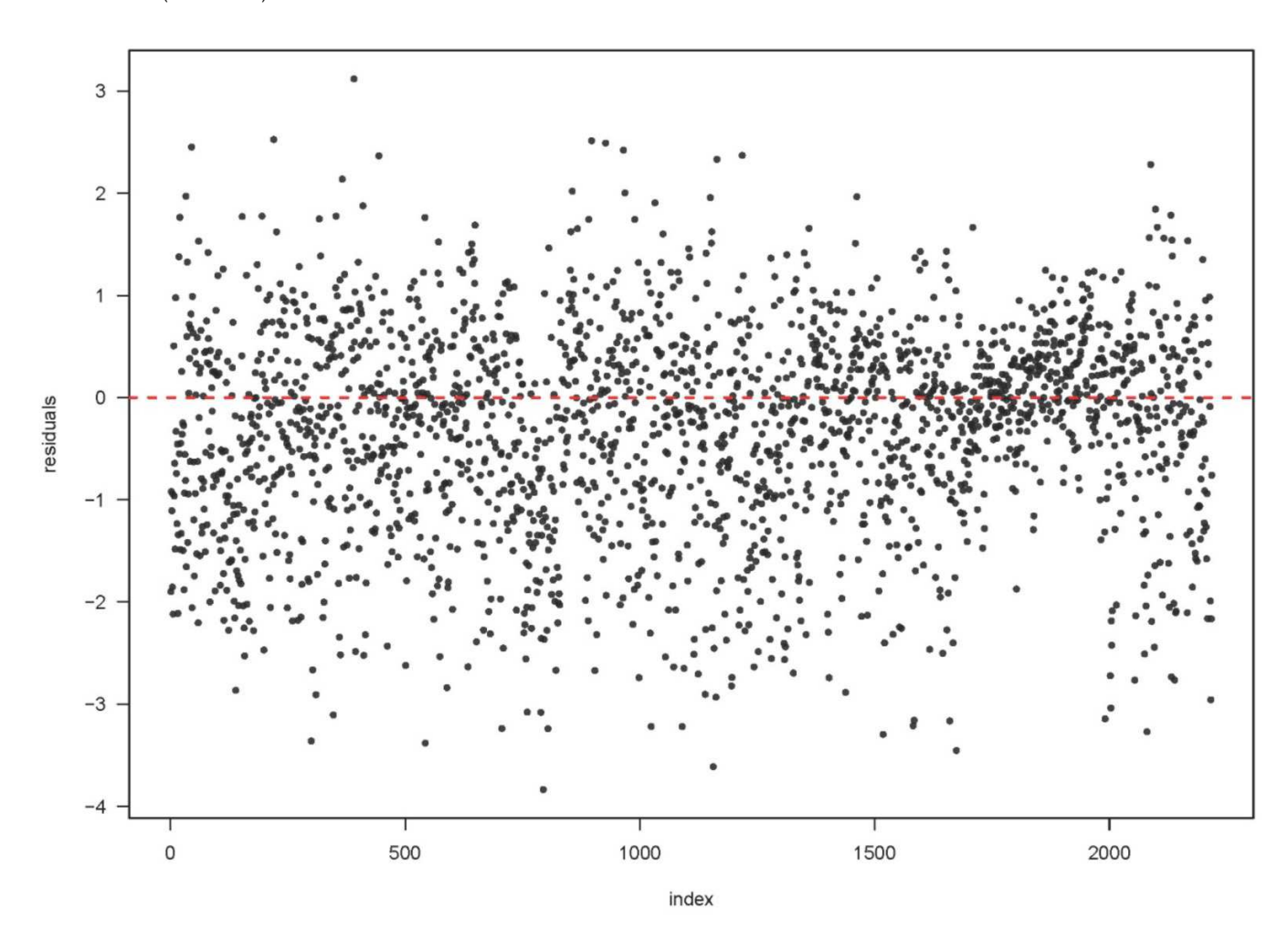


Fig. A2. The 80% prediction interval coverage probability for the quantile regression forest using the unconstrained estimate of aboveground live tree biomass carbon. The y-axis represents the difference in Mg C ha⁻¹ between predicted and observed biomass from the quantile regression forest (error, dashed line = 0 error). Grey bars represent the 80% prediction interval for each point estimate in the model.

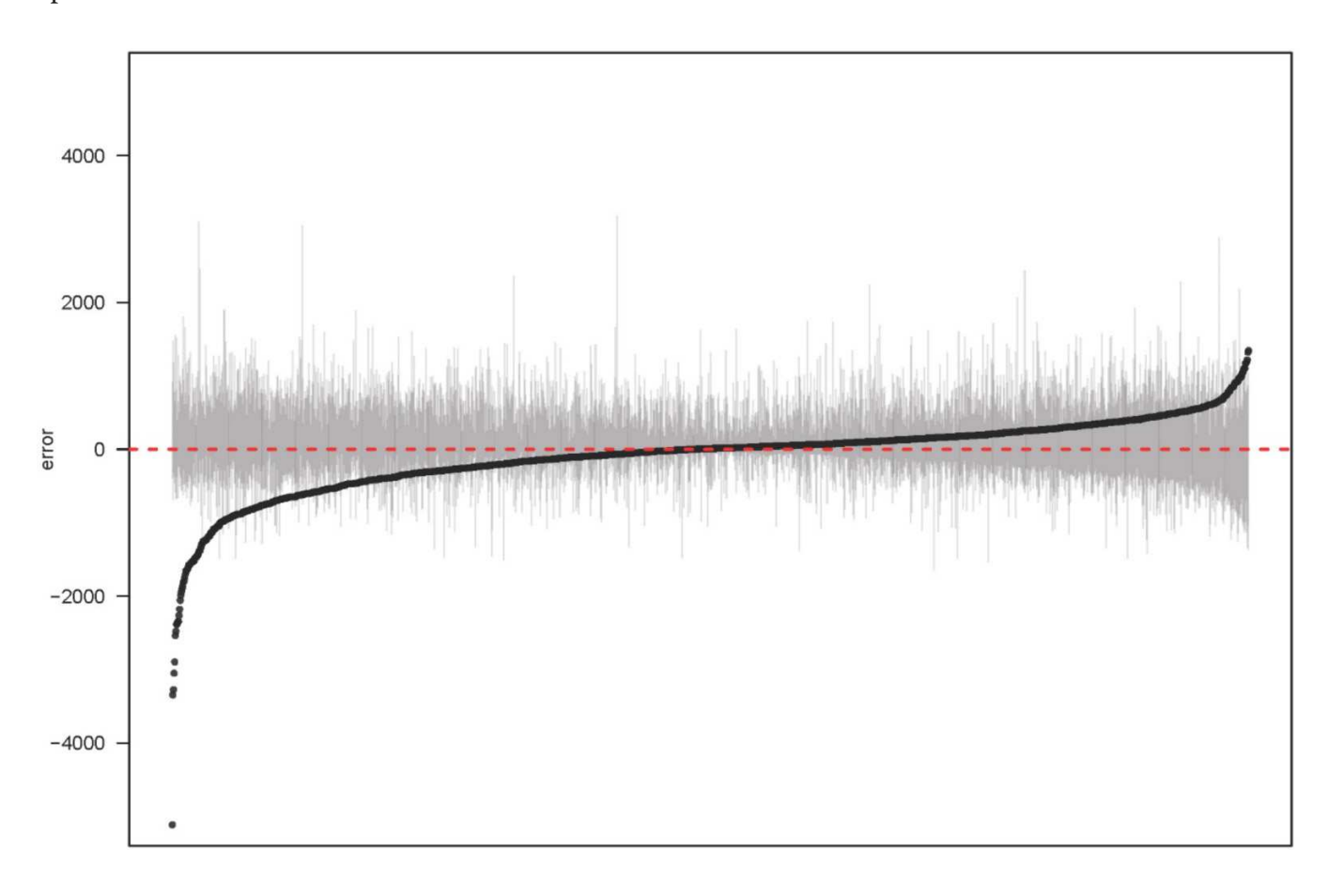


Fig. A3. Residuals of our generalized linear model after accounting for spatial autocorrelation plotted against individual covariates of our model. Spatial autocorrelation was not fully removed after including latitude and longitude in our model.

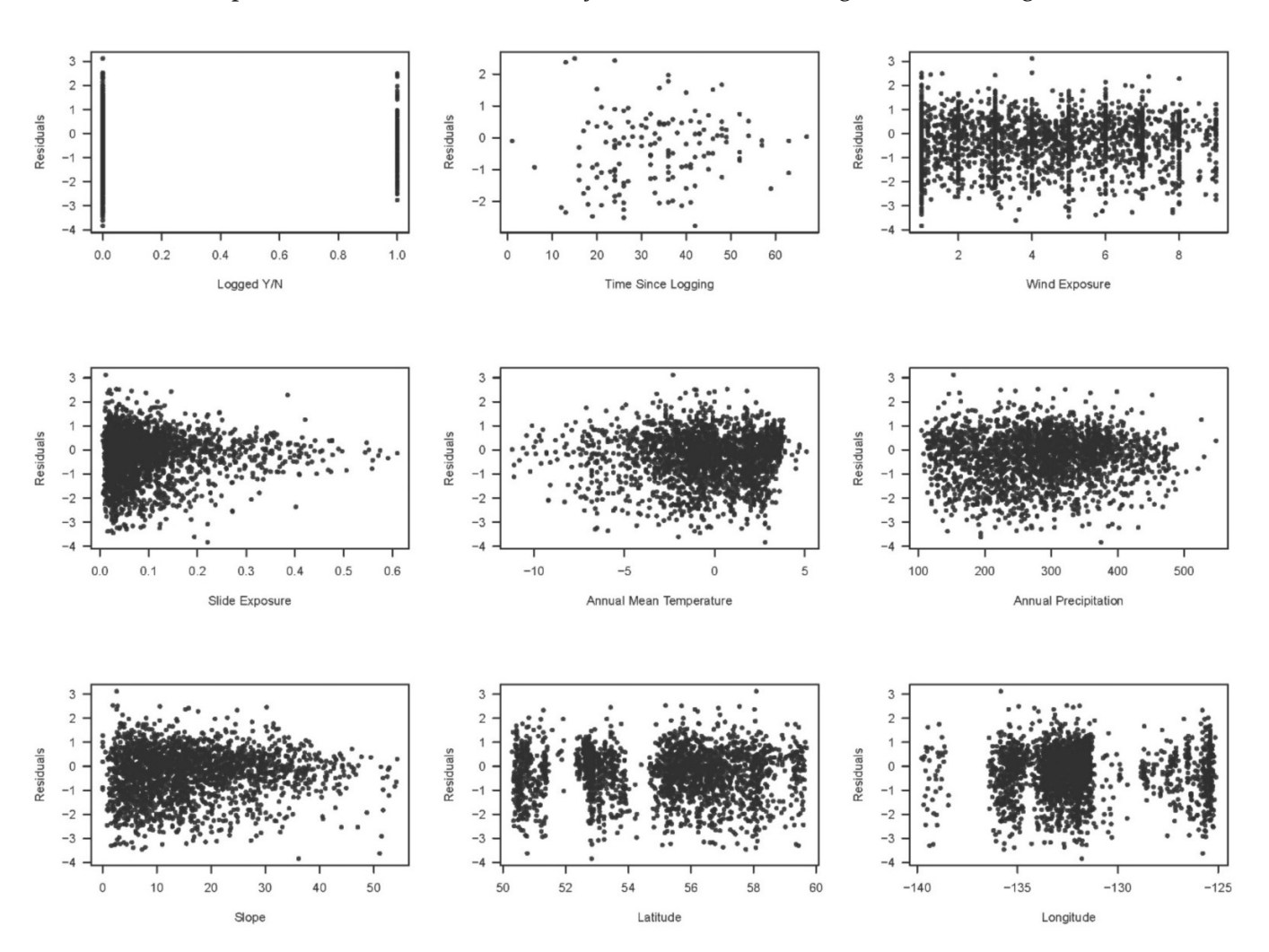


Fig. A4. The truncated estimate (n = 2218) of aboveground live tree biomass carbon for the perhumid ecoregion. Lighter orange and yellow colors indicate more aboveground live tree biomass. The mean aboveground live tree biomass for the perhumid ecoregion is 218 Mg ha⁻¹ and the maximum predicted tree biomass for the region is 2620 Mg ha⁻¹. Figure was created. ArcGIS Pro version 2.6.0 with data from the state of Alaska, Esri Canada, and USGS. Coordinate system is Alaska Albers equal area conic, datum WGS 1984, units in meters.

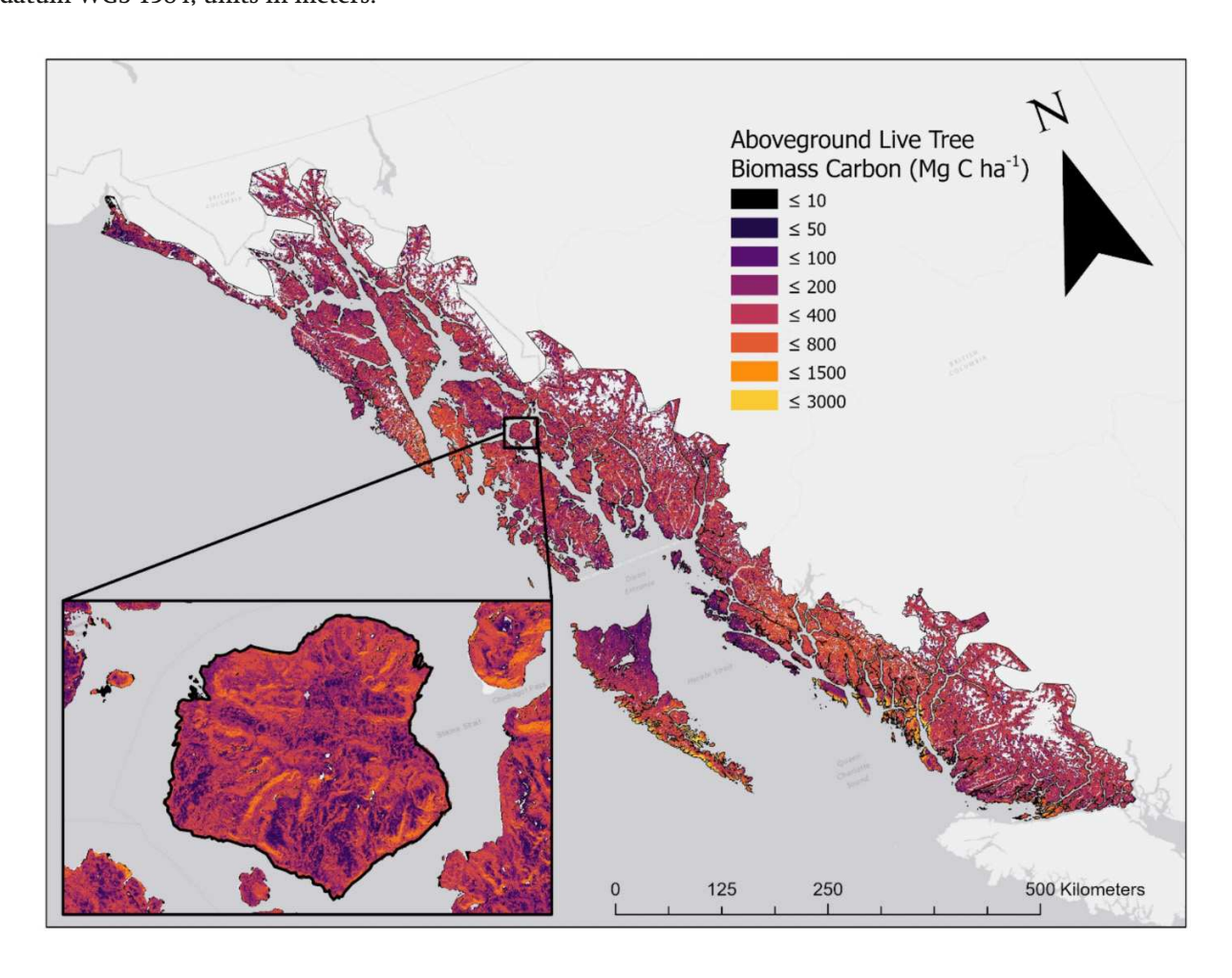


Fig. A5. The difference between the unconstrained estimate and truncated estimate (n = 2218 vs. n = 2218) of aboveground live tree biomass carbon. Purple and orange colors indicate where the full sample size estimate was larger, grey indicates zero change between estimates, and black represents areas where the biased estimate was larger than the full sample size estimate. On average, the full sample size estimate was 27% higher than the biased estimate. Figure was created using ArcGIS Pro version 2.6.0 with data from the state of Alaska, Esri Canada, and USGS. Coordinate system is Alaska Albers equal area conic, datum WGS 1984, units in meters.

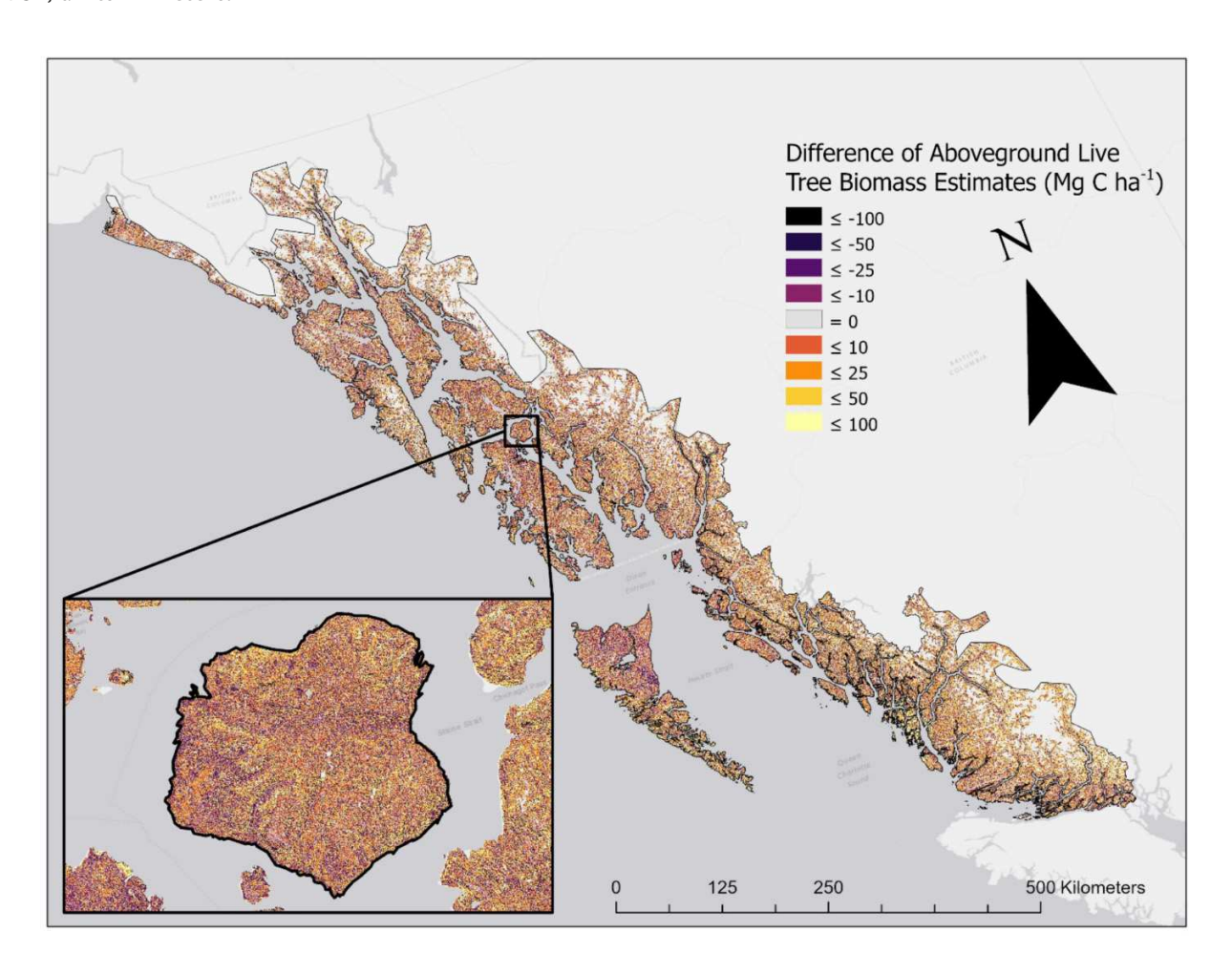


Fig. A6. The spatially explicit 80% prediction interval for the truncated estimate of aboveground live tree biomass carbon (Mg C ha^{-1}). The prediction interval coverage probability is 80.23% while 77.36% of predictions are within the prediction interval. The mean prediction interval (non-spatially explicit) was 1061 Mg C ha^{-1} while the median prediction interval (shown with dashed line) was 806 Mg C ha^{-1} . Figure was created using ArcGIS Pro version 2.6.0 with data from the state of Alaska, Esri Canada, and USGS. Coordinate system is Alaska Albers equal area conic, datum WGS 1984, units in meters.

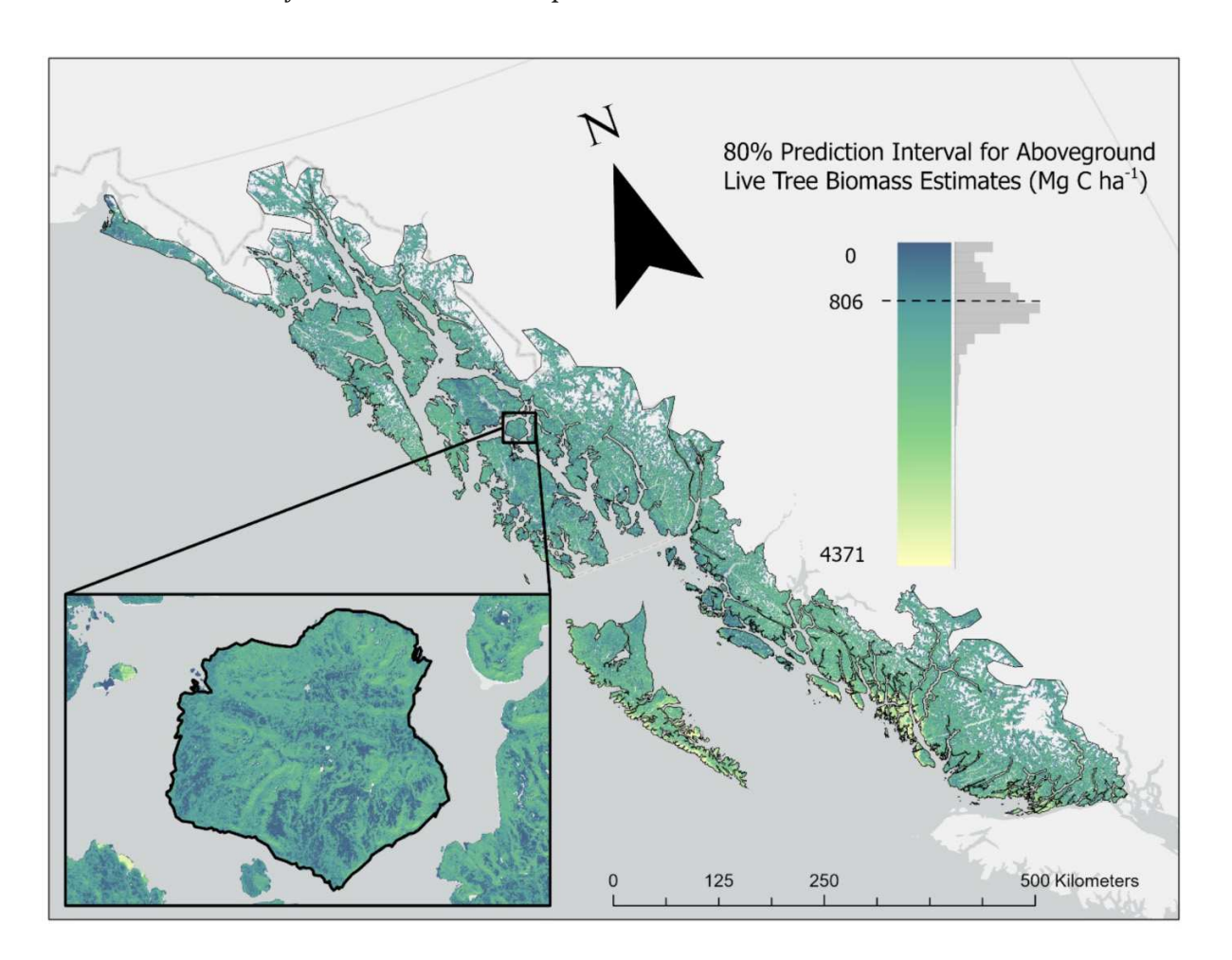


Table A3. Summary of the area disturbed or exposed to 1 disturbance (written as 1 disturbance in the table), disturbed and exposed to 1 disturbance or exposed to 2 disturbances (written as 2 disturbances in the table), or disturbed and exposed to 2 disturbances (written as 3 disturbances in the table) for southeast Alaska, coastal British Columbia and in total (AK + BC).

Disturbance	Area (ha)	Area (% of disturbed)
1 Disturbance	4 440 000	38.2%
2 Disturbances	3 360 000	29.0%
3 Disturbances	257 000	2.21%
Total Disturbed	8 060 000	69.5%
1 Disturbance AK	1 970 000	24.5%
1 Disturbance BC	2460000	30.6%
2 Disturbances AK	1 540 000	19.1%
2 Disturbances BC	1 820 000	22.6%
3 Disturbances AK	170 000	2.10%
3 Disturbances BC	87 200	1.08%

Note: Area is reported both in hectares disturbed and as a percentage of forested area (11.6 million ha).

Fig. A7. Variation in the sampling distribution for the mean of precipitation (a, e, and i), slope (b, f, and j), elevation (d, h, and l), and sample of aspect (c, g, and k) for logged and unlogged areas (a, b, c, and d), high and low relative frequency of windstorm disturbance regime (i.e., exposure; e, f, g, and h), and high and low relative frequency of landslide disturbance regime (i.e., exposure; i, j, k, and l). High and low relative frequencies for disturbance regimes are greater than or equal to the 70th percentile and lower than the 70th percentile of disturbance respective exposures. Results are not sensitive to arbitrary cutoff (data not shown).

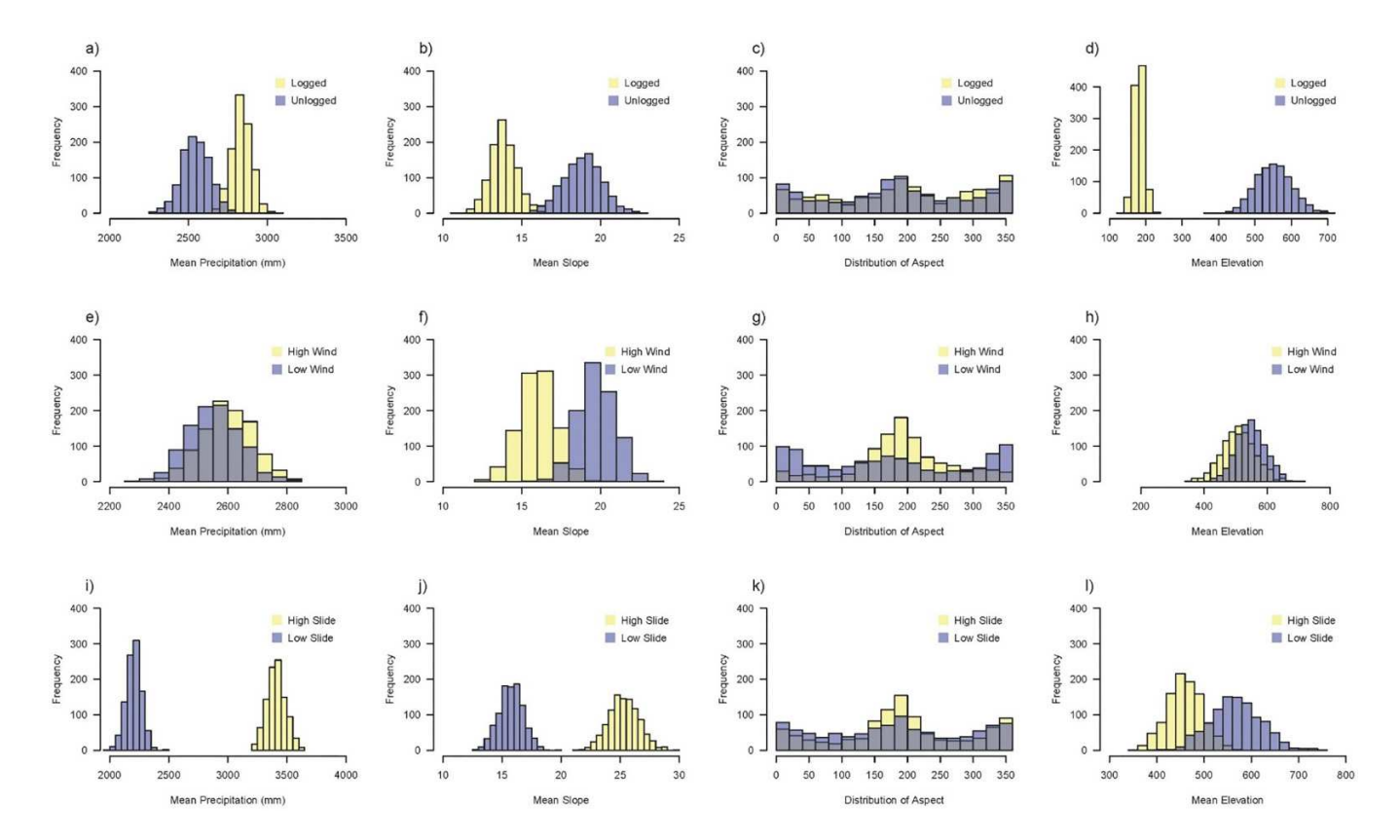


Fig. A8. Comparison of (*a*) mean sampling distributions for logged and unlogged areas across a gradient of the relative frequency of windstorm disturbance regimes. (*b*) The mean sampling distribution for high and low relative frequencies for land-slide disturbance regimes along a gradient of relative frequency for windstorm disturbance regimes. (*c*) The mean sampling distribution for logged and unlogged areas across a gradient of relative frequency for landslide disturbance regimes. (*d*) The mean sampling distribution for high and low relative frequencies for windstorm disturbance regimes along a gradient of relative frequency for landslide disturbance regimes. High relative frequency for a disturbance regime is >70th percentile of exposure for respective disturbance while low relative frequency \leq 70th percentile of exposure. Results are not sensitive to arbitrary cutoff (data not shown).

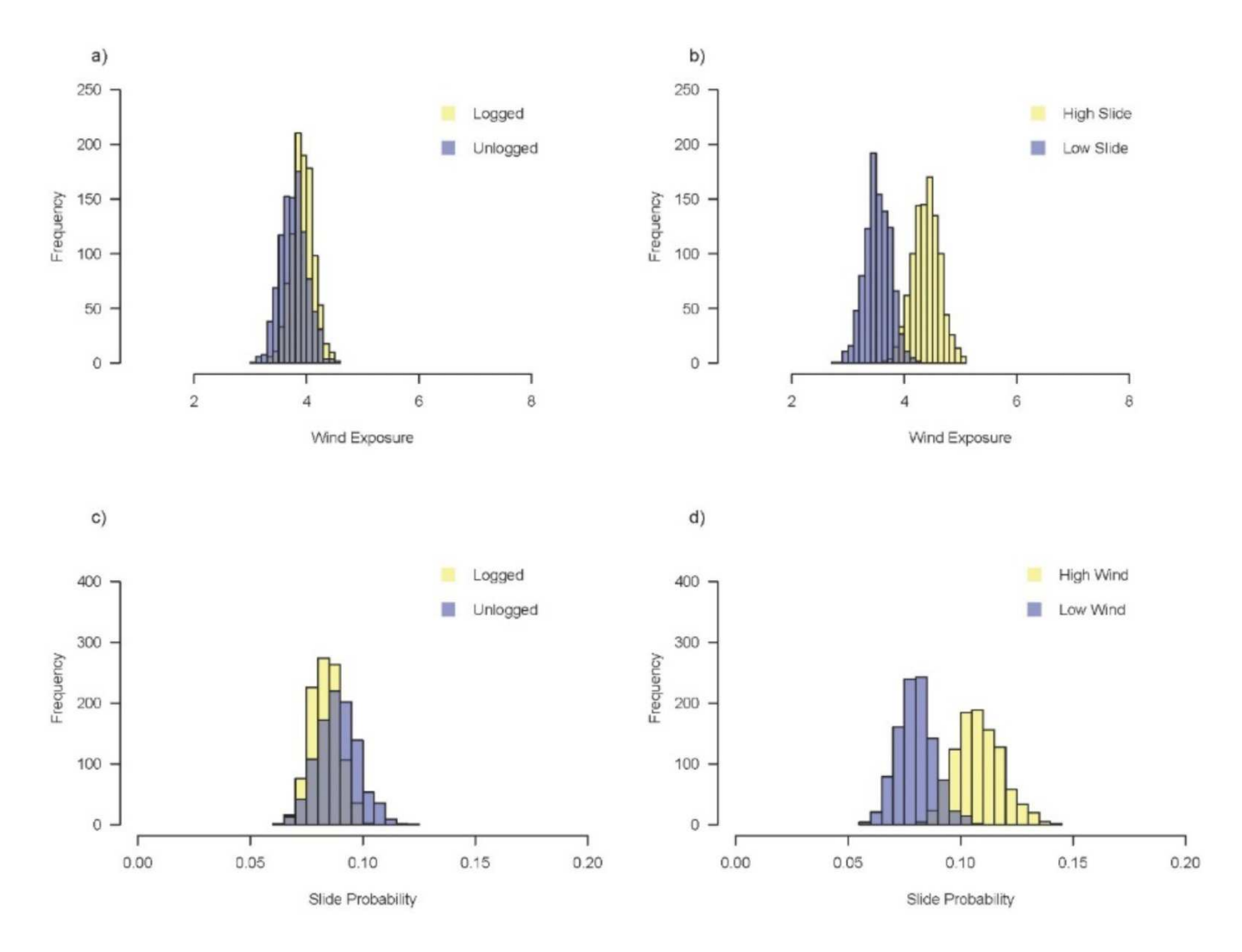


Fig. A9. Comparisons of aboveground live tree biomass carbon (Mg C ha $^{-1}$) in southeast Alaska (gold; AK) and coastal British Columbia (blue; BC) in plots that were unlogged (darker shade) as compared to logged (lighter shade). Logging corresponded with decreased average aboveground live tree biomass carbon in southeast Alaska with unlogged plots having 461 \pm 22 Mg C ha $^{-1}$ (mean \pm 95% CI) and logged plots having 189 \pm 49 Mg C ha $^{-1}$ (mean \pm 95% CI), as well as decreased average aboveground live tree biomass carbon in coastal BC with unlogged plots having 1074 \pm 59 Mg C ha $^{-1}$ (mean \pm 95% CI) and logged plots having 160 \pm 47 Mg C ha $^{-1}$ (mean \pm 95% CI). Each point represents a permanent sample plot for the respective dataset.

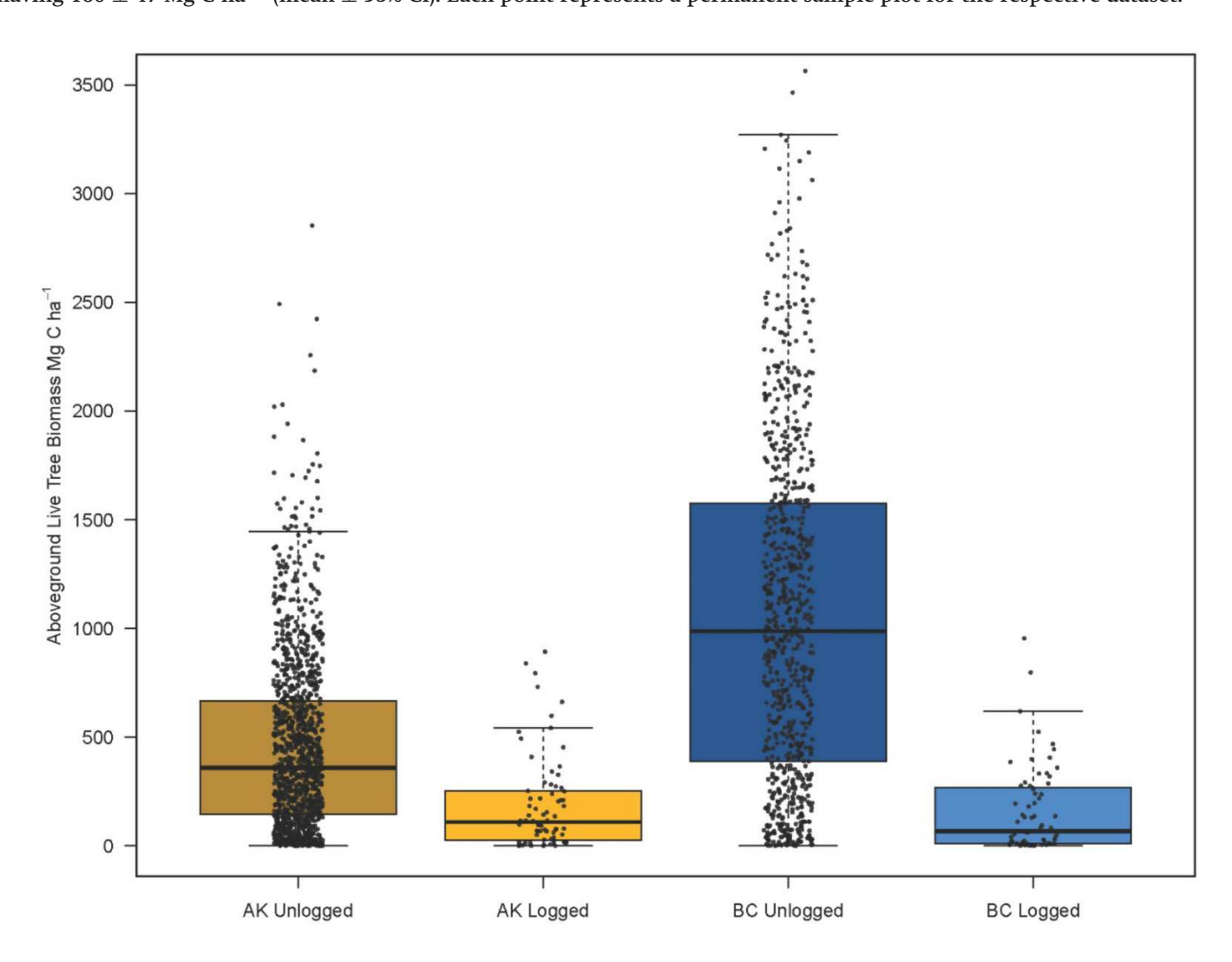


Fig. A10. Aboveground live tree biomass carbon of logged plots varying as a function of time since logging. At the lowest time since logging (1 year) aboveground live tree biomass carbon is on average 7.0 ± 6.3 Mg C ha⁻¹ (mean \pm 95% CI) while at the longest time since logging (67 years) aboveground live tree biomass carbon is on average 579 ± 484 Mg C ha⁻¹ (mean \pm 95% CI). The solid black line is the best fit regression line time since logging on aboveground live tree biomass carbon (Mg C ha⁻¹) from the model presented in Table 2. The shaded polygon represents the 95% confidence interval. Country of origin is displayed using squares for southeast Alaska and circles for coastal BC.

